ELSEVIER

Journal of Organometallic Chemistry 488 (1995) 29–38

Journal of Organometallic Chemistry

Instability of 15-electron Cp^*MoCl_2L (L = 2-electron donor) derivatives. X-ray structure of $Cp^*MoCl_2(PMe_2Ph)_2$ and $[Cp^*MoCl_2(PMe_2Ph)_2]AlCl_4$ ☆

Fatima Abugideiri [a], D. Webster Keogh [a], Heinz-Bernhard Kraatz [a], Wayne Pearson [b], Rinaldo Poli [a,*]

[a] *Department of Chemistry and Biochemistry, University of Maryland, College Park, MD 20742, USA*
[b] *Department of Chemistry, US Naval Academy, Annapolis, MD 21402, USA*

Received 17 March 1994

Abstract

The complex $Cp^*MoCl_2(PMe_2Ph)_2$ ($Cp^* = \eta^5C_5Me_5$) has been obtained in good yields from Cp^*MoCl_4, PMe_2Ph_2, and Na in the appropriate stoichiometric ratio, and it is also obtained by a ligand redistribution process after reduction of $Cp^*MoCl_3(PMe_2Ph)$ with Na. This compound is oxidized by the CH_2Cl_2 solvent in the presence of $AlCl_3$ to afford the salt $[Cp^*MoCl_2(PMe_2Ph)_2]AlCl_4$. Both compounds have been characterized crystallographically and by ^{1}H-NMR spectroscopy. The reasons for the instability of 15-electron Cp^*MoCl_2L complexes are discussed. The ^{1}H-NMR resonance data for $Cp^*MoCl_2L_2$ (L = PMe_3, PMe_2Ph) and $[Cp^*MoCl_2(PMe_2Ph)_2]^+$ are also discussed.

Keywords: Molybdenum; Crystal structure; Cyclopentadienyl

1. Introduction

Paramagnetic cyclopentadienyl-containing Mo(III) complexes are represented by the allyl complexes $CpMo(\eta-C_3H_5)_2$ and indenyl analogues [1], by the diene complexes $CpMoX_2(\eta^4$-diene) (X = halogen or thiolato group) [2], and by phosphine complexes of general formula $YMoX_2L_2$ (Y = cyclopentadienyl ring or substituted analogue, X = halogen, L = tertiary phosphine) [3–8]. All these compounds have 17 valence electrons. On the other hand, the lighter Group 6 ion, Cr(III), forms Cp half-sandwich derivatives predominantly having the 15-electron configuration. Examples are a variety of $CpCrX_2L$ (X = halogen, L = 2-electron donor) complexes [9], $[(C_5R_5)CrX(\mu-X)]_2$ (R = H, Me, X = halogen [9a,10] $[Cp^*CrR(\mu-X)]_2$ (X = halogen, R = alkyl) and their adducts with 2-electron donors L, Cp^*CrXRL [11]. A rare example of 17-electron Cp-substituted Cr(III) complexes is $CpCr(\eta-C_3H_5)_2$ [12]. The Cr(III) 15-electron materials show no tendency to add an additional ligand to reach a 17-electron configuration, but rather prefer in some cases to establish dissociation equilibria with 13-electron species [13].

We wondered whether a Cp-containing 15-electron Mo(III) complex could be sterically stabilized. A relevant point is that 15-electron complexes of formula MoX_3L_3 (X = halogen, L = neutral 2-electron donor) are a well-established class of compounds [14] and that the XL_2 ligand system is sterically more encumbering than the isoelectronic Cp ligand. We therefore attempted to synthesize sterically more congested Mo(III) derivatives by using the pentamethylcyclopentadienyl (Cp^*) ligand and bulky tertiary phosphines. This strategy recently proved successful in our laboratory for stabilizing corresponding electronically unsaturated half-sandwich Mo(IV) complexes [15]; whereas $CpMoCl_3L_n$ complexes with both $n = 1$ (16-electron) and $n = 2$ (18-electron) can be observed for L = PMe_3 and PMe_2Ph, only the unsaturated mono-L adduct can be obtained when L = $PMePh_2$. Only mono-L adducts can

☆ Dedicated to Professor Fausto Calderazzo on occasion of his 65th birthday, with gratitude.

* Corresponding author and Presidential Young Investigator 1900–1995, Alfred P. Sloan Research Fellow 1992–1994.

SSDI 0022-328X(94)00005-1

also be obtained for the Cp* system, Cp^*MoCl_3L (L = PMe_3, PMe_2Ph, $PMePh_2$).

The only Cp*Mo(III) compounds reported to date appear to be the 17-electron $Cp^*MoX_2(PMe_3)_2$ (X = Cl, I) [4,16] complexes, which show no evidence of ligand dissociation to afford 15-electron derivatives. We report here our studies of Cp*Mo systems with sterically more encumbering phosphines than PMe_3, which demonstrate the intrinsic instability of Cp^*MoCl_2L complexes toward a ligand redistribution reaction. Structural and spectroscopic studies of $Cp^*MoCl_2(PMe_2Ph)_2$ and of its one-electron oxidation product, unexpectedly obtained by the interaction of the Mo(III) precursor with the Lewis acid $AlCl_3$, are also reported and discussed.

2. Experimental details

All operations were carried out under argon. Solvents were dehydrated by standard methods and distilled directly from the dehydrating agent prior to use. The ^{1}H-NMR spectra were obtained with Bruker WP200 and AF200 spectrometers; the peak positions are reported downfield from TMS as calculated from the residual solvent peaks. EPR spectra were recorded on a Bruker ER200 spectrometer equipped with an X-band microwave generator. Cyclic voltammograms were recorded with an EG&G 362 potentiostat connected to a Macintosh computer through MacLab hardware/software; the electrochemical cell was a locally modified Schlenk tube with a Pt counter electrode sealed through uranium glass/Pyrex glass seals. The cell was fitted with a Ag/AgCl reference electrode and a Pt working electrode. All measurements were carried out in CH_2Cl_2 solutions with n-Bu_4NPF_6 (ca. 0.1 M) as supporting electrolyte. Potentials are reported vs. the Cp_2Fe/Cp_2Fe^+ couple, which was introduced into the cell at the end of each measurement. The elemental analyses were by M-H-W Laboratories, Phoenix, Arizona or Galbraith Laboratories, Inc., Knoxville, TN. Cp^*MoCl_4 was prepared by the standard PCl_5 method [17], although $[Cp^*Mo(CO)_3]_2$ and two equivalents of PCl_5 were used rather than $Cp^*Mo(CO)_3(CH_3)$ and 2.5 equivalents of PCl_5 (yield 97% on a 20 g scale). $[Cp^*MoCl_2]_2$ [18] and $Cp^*MoCl_3(PMe_2Ph)$ [15] were prepared as previously described.

2.1. Reaction between Cp^*MoCl_4, PMe_2Ph and Na in a 1:2:2 ratio. Synthesis of $Cp^*MoCl_2(PMe_2Ph)_2$

Into a Schlenk tube were introduced, in turn, sodium amalgam (66.2 mg, 2.88 mmol in 17 g of Hg), Cp^*MoCl_4 (537 mg, 1.44 mmol), 40 mL of THF, and PMe_2Ph (410 μL, 398 mg, 2.88 mmol). The resulting mixture was magnetically stirred at room temperature for 3 days, after which it was filtered through Celite and evaporated to dryness. The residue was extracted with toluene (20 mL) and the extract was filtered, and evaporated to dryness to afford 785 mg (94%) of product, which was recrystallized from cold pentane. Anal. calc. for $C_{26}H_{37}Cl_2MoP_2$: C, 53.99; H, 6.44. Found: C, 54.2; H, 6.3%. ^{1}H-NMR (C_6D_6): 10.4 (br s, $w_{1/2}$ = 40 Hz); 7.9 (br s, $w_{1/2}$ = 100 Hz); 2.4 (br s, $w_{1/2}$ = 40 Hz); −2.1 (br s, $w_{1/2}$ = 120 Hz). This spectrum is shown in Fig. 1, and a tentative assignment of the NMR resonances is given in Section 3. EPR in n-heptane gives no signal at room temperature, but a feature appears upon cooling to 220 K and becomes a distinguishable triplet at 190 K: g = 1.988, a_P = 13.4 G. However, the line width is still too large for the Mo satellites (^{95}Mo + ^{97}Mo, both with I = 5/2, total abundance: 25.2%) to be discernible. At T < 190 K, the EPR resonance becomes a broad singlet again. Cyclic voltammogram: −0.91 V (reversible oxidation); +0.88 (reversible oxidation). A single crystal obtained from pentane was used for the X-ray study (vide infra).

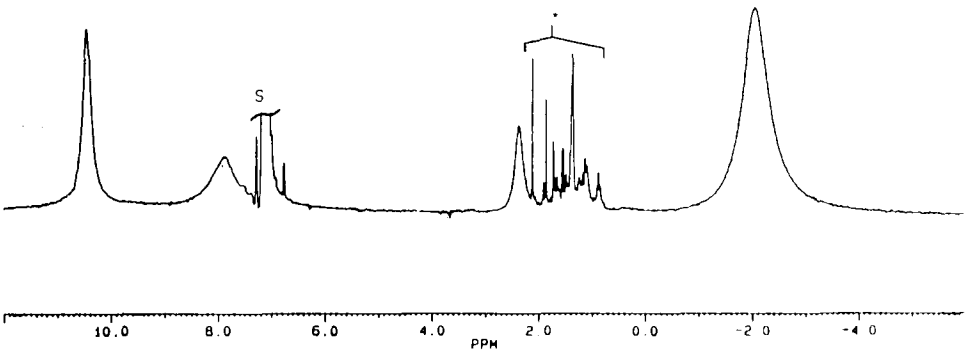

Fig. 1. Room temperature ^{1}H-NMR spectrum of $Cp^*MoCl_2(PMe_2Ph)_2$. S = residual proton resonance of the NMR solvent (C_6D_6). * = crystallization solvents and other unknown diamagnetic impurities.

2.2. Reaction between $Cp^*MoCl_3(PMe_2Ph)$ and Na. Formation of $Cp^*MoCl_2(PMe_2Ph)_2$ and $[Cp^*MoCl_2]_2$

$Cp^*MoCl_3(PMe_2Ph)$ (213 mg, 0.448 mmol) was added to a Schlenk tube containing sodium amalgam (10.3 mg of Na, 0.448 mmol, in 21.8 g of Hg) and 30 mL of THF. The mixture was stirred magnetically for ca. 24 h and then filtered through Celite. An aliquot of the solution was evaporated to dryness and the residue dissolved in C_6D_6; the NMR spectrum of the solution showed the presence of $[Cp^*MoCl_2]_2$ (δ 1.70, by comparison with an authentic sample) and paramagnetically shifted resonances of $Cp^*MoCl(PMe_2Ph)_2$ (vide supra).

2.3. Reaction between $[Cp^*MoCl_2]_2$ and PR_3 (one equivalent)

2.3.1. $PR_3 = PMe_3$

Into a Schlenk tube were introduced, in turn, $[Cp^*MoCl_2]_2$ (184 mg, 0.305 mmol), toluene (30 mL) and PMe_3 (63 μL, 0.61 mmol). The resulting mixture was magnetically stirred overnight. At this point, an aliquot of the solution was evaporated to dryness and the residue was dissolved in C_6D_6; the ^{1}H-NMR spectrum of the solution showed the presence of unchanged $[Cp^*MoCl_2]_2$ (δ 1.70) and a broad resonance at δ −2.4, which is assigned to $Cp^*MoCl_2(PMe_3)_2$ by comparison with data for an authentic sample [16]. A similar experiment was also carried out in THF, and identical behavior was observed, that is formation of $Cp^*MoCl_2(PMe_3)_2$ with part of the starting material remaining unchanged.

2.3.2. $PR_3 = PMe_2Ph$

By analogy with reaction 2.3.1. above, the interaction between $[Cp^*MoCl_2]_2$ and PMe_2Ph in a 1:2 molar ratio in THF gave rise to $Cp^*MoCl_2(PMe_2Ph)_2$, recognized by the ^{1}H-NMR spectrum (see above and Fig. 1) and unreacted $[Cp^*MoCl_2]_2$.

2.3.3. $PR_3 = PMePh_2$

Into a Schlenk tube were introduced $[Cp^*MoCl_2]_2$ (344 mg, 0.570 mmol), THF (40 mL) and $PMePh_2$ (212 mL, 1.14 mmol). After magnetic stirring at room temperature overnight, an aliquot was evaporated to dryness and the residue was dissolved in C_6D_6; the NMR spectrum of the solution showed only unchanged starting materials.

2.4. Reaction between $Cp^*MoCl_2(PMe_3)_2$ and $BH_3 \cdot THF$

$Cp^*MoCl_2(PMe_3)_2$ (384 mg, 0.84 mmol) was introduced into a Schlenk tube along with 30 mL of THF and $BH_3 \cdot THF$ (0.84 mL of a 1.0 M solution, 0.84 mmol). The solution was magnetically stirred for 2 days at room temperature. An aliquot of the solution was then evaporated to dryness, the residue was redissolved in C_6D_6, and the solution was examined by NMR spectroscopy. ^{1}H-NMR: a resonance at δ 1.70 was assigned to $[Cp^*MoCl_2]_2$ and a broad ($w_{1/2} = 90$ Hz) resonance at δ −2.4 was assigned to $Cp^*MoCl_2(PMe_3)_2$, based on comparisons with the spectra of authentic samples. $PMe_3 \cdot BH_3$ was identified by a ^{1}H-NMR resonance at δ 0.61 (d, $J_{HP} = 9.7$ Hz) and by a $^{31}P\{^1H\}$-NMR resonance at δ −165.5 (q, $J_{PB} = 57.5$ Hz).

2.5. Reaction of $Cp^*MoCl_2(PMe_2Ph)_2$ with $AlCl_3$. Preparation of $[Cp^*MoCl_2(PMe_2Ph)_2]AlCl_4$

Into a Schlenk tube equipped with a magnetic stir bar were introduced, in turn, $Cp^*MoCl_2(PMe_2Ph)_2$ (150 mg, 0.259 mmol), $AlCl_3$ (34.6 mg, 0.259 mmol) and CH_2Cl_2 (20 mL). The solution was initially red-brown, and white $AlCl_3$ remained undissolved. Stirring at room temperature caused a color change to deep red, and the dissolution of $AlCl_3$ within 15 min. After filtration, the solution was reduced in volume to ca. 5 mL and layered with *n*-heptane (10 mL). Diffusion of the two layers at room temperature during one week afforded red crystals, which were isolated by decanting off the mother liquor and dried under vacuum (121 mg, 62.5% yield). Anal. calc. for $C_{26}H_{37}AlCl_6MoP_2$: C, 41.79; H, 4.99; Cl, 28.47. Found: C, 40.7; H, 5.1; Cl, 30.1%. The low C and high Cl analyses may be the result of co-crystallization of some $Al_2Cl_7^-$ salt with the main $AlCl_4^-$ product. The crystals appeared homogeneous by optical inspection. A crystal from this batch was used for an X-ray study (vide infra). ^{1}H-NMR ($CDCl_3$, δ): broad overlapping peaks in the δ 15-11 region [main peak at 11.6 ($w_{1/2}$ = ca. 100 Hz) with shoulders at ca. 12.5 ($w_{1/2}$ = ca. 400 Hz) and ca. 14.5 ($w_{1/2}$ = ca. 500 Hz)], 3.4 (br s, $w_{1/2} = 100$ Hz), −6 (very broad, $w_{1/2}$ = ca. 600 Hz).

2.6. X-ray crystallography

2.6.1. $Cp^*MoCl_2(PMe_2Ph)_2$

A suitable crystal was mounted in a random orientation on a glass fiber. Rotation photographs were used to locate reflections which were then indexed to obtain the unit cell for the crystal. The initial unit cell appeared to be monoclinic. Axial photographs confirmed axial lengths for the unit cell and mirror symmetry with respect to a single axis. Conditions for reflection ($h0l$ $= 2n$ and $0k0$ $k = 2n$) were the only restrictions on reflection class and allowed the assignment of space group $P2_1/c$. A linear decay correction was applied to the data set. The empirical absorption correction was based on ψ scans of three reflections at 10° intervals.

The structure was solved by direct methods and completed with difference Fourier syntheses. All non-hydrogen atoms were refined with anisotropic temperature factors. Hydrogen atoms were located in the difference Fourier maps for the methyl and phenyl groups, and refined with isotropic temperature factors. Hydrogens on the Cp* ring were placed at idealized positions and assigned a temperature factor 30% larger than the corresponding carbon isotropic temperature factor. Hydrogen positions were updated through the final cycles of refinement. A number of weighting schemes were attempted with the lowest R factor and Goodness of Fit obtained with unit weights with a 3σ cut-off on structure factors. Examination of strong, low-angle reflections revealed no extinction effects.

Difference Fourier maps on the Cp* ring revealed a high degree of libration for the ring. Initial attempts to refine a single ring resulted in $wR(F)$ of 0.034 with considerable density remaining in the ring. A second attempt was made to model the ring with two Cp* rings with variable multiplicities. This model led to multiplicities of 0.618 and 0.382 for the two rings and a final $wR(F)$ of 0.023. Owing to the large degree of correlation between the two rings, one ring was refined while the other was fixed. Successive iterations, involving refinement of alternate rings, led to the final structure. Selected crystal data are collected in Table 1, positional and equivalent isotropic thermal parameters are listed in Table 2, and selected bond distances and angles are in Table 3.

2.6.2. $[Cp^*MoCl_2(PMe_2Ph)_2]AlCl_4$

A single crystal was mounted under dinitrogen in a thin-walled glass capillary, which was then flame sealed and mounted on the diffractometer. A least-squares fit on the setting angles of 25 reflections with $23° < 2\theta < 32.5°$ gave a monoclinic unit cell. Systematic absences from the data set uniquely established the space group as $P2_1/n$. The periodic monitoring of three standard reflections indicated no significant variation of intensity. The data were corrected for Lorentz and polarization effects and an absorption correction based on 7 ψ scans at 10° intervals was also applied. The structure was solved by direct methods (MITHRIL), which revealed the location of the Mo, Al and all of the Cl and P atoms, and was subsequently refined by alternate full-matrix least-squares cycles and difference Fourier syntheses, which revealed the position of the other non-hydrogen atoms. The hydrogen atoms were included at calculated positions and used for structure factor calculations but not refined. Selected crystal data are listed in Table 1, positional and equivalent isotropic thermal parameters are in Table 4, and selected bond distances and angles are in Table 3. Complete lists of bond lengths and angles, and tables of hydrogenatom coordinates and anisotropic thermal parameters have been deposited at the Cambridge Crystallographic Data Centre.

3. Results and discussion

The Mo(III) complex $Cp^*MoCl_2(PMe_2Ph)_2$ is obtained in a straightforward manner by reduction of Cp^*MoCl_4 with two equivalents of sodium in the presence of two equivalents of PMe_2Ph (Eqn. 1), but it can also be prepared by addition of the phosphine to the pre-formed product of reduction, i.e. $[Cp^*MoCl_2]_2$. The addition of only one equivalent of the phosphine per Mo to $[Cp^*MoCl_2]_2$ results in the formation of the same *bis*-PMe_2Ph product, leaving part of the starting material unreacted (Eqn. 2). The same phenomenon is

Table 1
Crystal data for all compounds

Compound	$Cp^*MoCl_2(PMe_2Ph)_2$	$[Cp^*MoCl_2(PMe_2Ph)_2]AlCl_4$
Formula	$C_{26}H_{37}Cl_2MoP_2$	$C_{26}H_{37}AlCl_6MoP_2$
fw	578.37	747.17
Space group	$P2_1/c$	$P2_1/n$
a, Å	9.5295(4)	18.617(3)
b, Å	13.426(1)	8.935(2)
c, Å	21.488(3)	20.749(4)
β, deg	97.26(3)	93.93(2)
V, Å^3	2721(1)	3444(2)
Z	4	4
d_{calc}, g cm^{-3}	1.409	1.44
μ(Mo–Kα), cm^{-1}	7.946	9.70
Radiation (monochromated in incident beam)	Mo–Kα (λ = 0.71073 Å)	Mo–Kα (λ = 0.71073 Å)
Temp, °C	25	23
T (max)/T (min)	1.05	1.20
R [a]	0.021	0.046
R_w [b]	0.023	0.062

[a] $R = \Sigma \| F_o \| - | F_c \| / \Sigma | F_o |$. [b] $R_w = [\Sigma w(| F_o | - | F_c |)^2 / \Sigma w | F_o |^2]^{1/2}$; $w = 1/\sigma^2(| F_o |)$.

observed upon addition of PMe_3 (with formation of 17-electron $Cp^*MoCl_2(PMe_3)_2$), whereas the addition of the bulkier phosphine $PMePh_2$ does not result in any reaction, showing that the $Cp^*MoCl_2(PMe_2Ph)_2$ is sterically as congested as this system can tolerate. With the less encumbering Cp ring, on the other hand a 17-electron adduct was also obtained with the bulkier triphenylphosphine, $CpMoCl_2(PPh_3)$ [7]. There is no evidence for the formation of a 15-electron monophosphine adduct, Cp^*MoCl_2L.

$$Cp^*MoCl_4 + 2Na + 2PMe_2Ph \longrightarrow Cp^*MoCl_2(PMe_2Ph)_2 + 2NaCl \quad (1)$$

$$[Cp^*MoCl_2]_2 + 2L \longrightarrow 2\{Cp^*MoCl_2L\} \longrightarrow 1/2[Cp^*MoCl_2]_2 + Cp^*MoCl_2L_2 \quad (2)$$

There is again no accumulation of a 15-electron Cp^*MoCl_2L adduct (with $L = PMe_3$) when the *bis*-phosphine compound is treated with one equivalent of

Table 2
Positional parameters and equivalent isotropic thermal parameters for $Cp^*MoCl_2(PMe_2Ph)_2$

Atom	x	y	z	B(A2)
Mo	0.30222(3)	0.13700(2)	0.63681(1)	3.180(5)
Cl1	0.3872(1)	0.28940(7)	0.69485(4)	4.78(2)
Cl2	0.08179(9)	0.03710(7)	0.63057(4)	4.87(2)
P1	0.12093(9)	0.26108(7)	0.58790(4)	3.97(2)
P2	0.30014(9)	0.08085(7)	0.74876(4)	3.94(2)
C1	0.0265(4)	0.3135(3)	0.6485(2)	5.8(1)
C2	−0.0249(4)	0.2143(3)	0.5330(2)	6.1(1)
C3	0.2738(4)	−0.0499(3)	0.7646(2)	5.8(1)
C4	0.4513(4)	0.1100(4)	0.8068(2)	6.3(1)
C5	0.6604(7)	0.1976(6)	0.6428(4)	8.6(2)
C6	0.4575(7)	0.2494(6)	0.5211(3)	8.7(2)
C7	0.2561(8)	0.0595(7)	0.4866(3)	8.4(2)
C8	0.3402(9)	−0.1022(5)	0.5903(4)	9.3(2)
C9	0.5987(8)	−0.0203(6)	0.6816(4)	8.9(2)
C10	0.5398(5)	0.1368(5)	0.6138(3)	4.6(1)
C11	0.4404(5)	0.1600(4)	0.5586(2)	3.5(1)
C12	0.3491(5)	0.0754(4)	0.5447(3)	4.2(1)
C13	0.3969(6)	0.0004(4)	0.5941(3)	5.0(1)
C14	0.5116(6)	0.0413(4)	0.6338(3)	4.5(1)
C15	0.1735(4)	0.3711(3)	0.5471(2)	4.19(8)
C16	0.2492(5)	0.4471(3)	0.5778(2)	7.2(1)
C17	0.2933(6)	0.5283(4)	0.5467(2)	9.2(1)
C18	0.2622(5)	0.5336(3)	0.4832(2)	7.9(1)
C19	0.1869(5)	0.4620(3)	0.4514(2)	7.0(1)
C20	0.1435(4)	0.3826(3)	0.4832(2)	5.8(1)
C21	0.1550(3)	0.1400(3)	0.7827(1)	4.09(8)
C22	0.1695(4)	0.2342(3)	0.8089(2)	5.6(1)
C23	0.0607(5)	0.2801(3)	0.8334(2)	7.4(1)
C24	−0.0645(5)	0.2333(4)	0.8326(2)	8.5(1)
C25	−0.0835(4)	0.1408(4)	0.8068(2)	7.5(1)
C26	0.0254(4)	0.0947(3)	0.7817(2)	5.5(1)
C5′	0.556	0.255	0.567	22.0
C6′	0.318	0.159	0.475	17.5
C7′	0.257	−0.052	0.524	13.2
C8′	0.457	−0.097	0.644	12.3
C9′	0.652	0.093	0.676	15.0
C10′	0.486	0.160	0.581	3.7
C11′	0.384	0.115	0.539	4.7
C12′	0.357	0.019	0.562	4.9
C13′	0.450	0.008	0.616	5.3
C14′	0.526	0.096	0.626	5.0

Anisotropically refined atoms are given in the form of the isotropic equivalent displacement parameter defined as: $(4/3)*[a^2*B(1,1)+b^2*B(2,2)+c^2*B(3,3)+ab(\cos\gamma)*B(1,2)+ac(\cos\beta)*B(1,3)+bc(\cos\alpha)*B(2,3)]$

Table 3
Selected bond distances (Å) and angles (°) for $Cp^*MoCl_2(PMe_2Ph)_2$ and for $[Cp^*MoCl_2(PMe_2Ph)_2]AlCl_4$

$Cp^*MoCl_2(PMe_2Ph)_2$		$[Cp^*MoCl_2(PMe_2Ph)_2]AlCl_4$	
	Distance		*Distance*
Mo–C11	2.4784(9)	Mo–C11	2.386(2)
Mo–C12	2.4816(9)	Mo–C12	2.380(2)
Mo–P1	2.5308(9)	Mo–P1	2.576(2)
Mo–P2	2.5235(9)	Mo–P2	2.556(2)
Mo–CNT [a]	1.966(5)	Mo–CNT [b]	2.034(9)
P1–C1	1.816(4)	P1–C11	1.798(9)
P1–C2	1.818(4)	P1–C12	1.810(9)
P1–C15	1.821(4)	P1–C13	1.821(8)
P2–C3	1.811(4)	P2–C21	1.795(9)
P2–C4	1.824(4)	P2–C22	1.81(1)
P2–C21	1.825(4)	P2–C23	1.80(1)
		Al–C13	2.098(5)
		Al–C14	2.124(5)
		Al–C15	2.110(4)
		Al–C16	2.113(4)
	Angle		*Angle*
C11–Mo–C12	133.94(3)	C11–Mo–C12	138.23(9)
C1–Mo–P1	80.10(3)	C11–Mo–P1	79.89(7)
Cl1–Mo–P2	78.95(3)	C11–Mo–P2	79.42(8)
C11–Mo–CNT [a]	111.2(1)	C11–Mo–CNT [b]	110.5(3)
C12–Mo–P1	78.74(3)	C12–Mo–P1	79.65(7)
C12–Mo–P2	77.37(3)	C12–Mo–P2	77.99(8)
C12–Mo–CNT [a]	114.8(1)	C12–Mo–CNT [b]	111.2(3)
P1–Mo–P2	120.35(3)	P1–Mo–P2	116.80(8)
P1–Mo–CNT [a]	121.0(1)	P1–Mo–CNT [b]	121.9(3)
P2–Mo–CNT [a]	118.6(1)	P2–Mo–CNT [b]	121.3(3)
Mo–P1–C1	109.4(1)	Mo–P1–C11	110.1(3)
Mo–P1–C2	117.9(1)	Mo–P1–C12	115.9(3)
Mo–P1–C15	121.3(1)	Mo–P1–C13	117.9(3)
C1–P1–C2	101.1(2)	C11–P1–C12	102.5(5)
C1–P1–C15	102.9(2)	C11–P1–C13	105.1(4)
C2–P1–C15	101.7(2)	C12–P1–C13	103.8(4)
Mo–P2–C3	119.1(1)	Mo2–P2–C21	117.1(3)
Mo–P2–C4	119.1(2)	Mo2–P2–C22	118.1(4)
Mo–P2–C21	110.4(1)	Mo2–P2–C23	108.5(3)
C3–P2–C4	101.3(2)	C21–P2–C22	102.3(5)
C3–P2–C21	102.5(2)	C21–P2–C23	105.3(5)
C4–P2–C21	101.9(2)	C22–P2–C23	104.1(5)
		Cl3–Al–Cl4	108.4(2)
		Cl3–Al–Cl5	111.2(2)
		Cl3–Al–Cl6	108.8(2)
		Cl4–Al–Cl5	106.8(2)
		Cl4–Al–Cl6	110.4(2)
		Cl5–Al–Cl6	111.4(2)

[a] Centroid of atoms C10–C14. [b] Centroid of atoms C31–C35.

the phosphine-scavenger compound $BH_3 \cdot THF$, the product of the reaction again being a mixture of the *bis*-phosphine adduct and $[Cp^*MoCl_2]_2$ (Eqn. 3). In this reaction, the formation of the phosphine-BH_3 adduct was confirmed by ^1H- and ^{31}P-NMR spectroscopy.

$$2Cp^*MoCl_2(PMe_3)_2 + 2BH_3 \cdot THF \xrightarrow[-THF]{-BH_3 \cdot PMe_3} 2\{Cp^*MoCl_2L\} \longrightarrow 1/2[Cp^*MoCl_2]_2 + Cp^*MoCl_2L_2 \quad (3)$$

It is possible that the absence of accumulation of a 15-electron complex in Eqns. 2 and 3 is due to kinetic reasons. In other words, it may be that Cp^*MoCl_2L reacts more rapidly than $[Cp^*MoCl_2]_2$ with phosphines, and more rapidly than $Cp^*MoCl_2L_2$ with $BH_3 \cdot THF$. These problems are eliminated by adopting the alternative strategy illustrated in Eqn. 4, involving reduction of the $Cp^*MoCl_3(PMe_2Ph)$ precursor that already contains the required L:Mo ratio at the molecular level in the starting material. However, such reaction again results in the formation of a mixture of $[Cp^*MoCl_2]_2$ and *bis*-phosphine complex. This result demonstrates that the hypothetical 15-electron $Cp^*MoCl_2(PMe_2Ph)$ complex is thermodynamically unstable toward a ligand redistribution to give the observed products. This transformation is also illustrated in Scheme 1.

$$2Cp^*MoCl_3(PMe_3) + 2Na \xrightarrow{-NaCl} 2\{Cp^*MoCl_2L\} \longrightarrow 1/2[Cp^*MoCl_2]_2 + Cp^*MoCl_2L_2 \quad (4)$$

It is not too difficult to suggest a rationalization for this result, and for the difference with respect to the corresponding Cr(III) chemistry. In the case of the Mo system, we know that $[Cp^*MoCl_2]_2$ has the quadruply-chloro-bridged structure depicted in the Scheme because this has been found by X-ray methods for the closely related $[(C_5H_4\text{-}i\text{-}Pr)MoCl_2]_2$ and $[(C_5Me_4Et)MoCl_2]_2$ complexes [3a,19]. Furthermore, the compound is diamagnetic in solution, in accord with the formation of a Mo–Mo bond which gives a formal 18-electron count to the metal centers. Therefore, according to the Scheme, the metal on the left-hand side of the equilibrium is bonded to only three monodentate ligands (two Cl and one L), whereas on the right-hand side, each metal forms four bonds to the monodentate ligands (two Cl and two L ligands in the mononuclear 17-electron compound and four bridging Cl ligands in the dinuclear complex). In addition, the dinuclear compound provides the additional driving force for the formation of the Mo–Mo bond. Therefore, the formation of a greater number of bonds drives the equilibrium toward the right. For the chromium system, on the other hand, there is a steric impediment to the coordination of four monodentate ligands to the smaller Cr(III) center, since 17-electron $CpCrCl_2L_2$ complexes do not exist and since the dinuclear $[CpCrCl_2]_2$ system adopts the geometry shown in the Scheme where each metal is bonded to only three

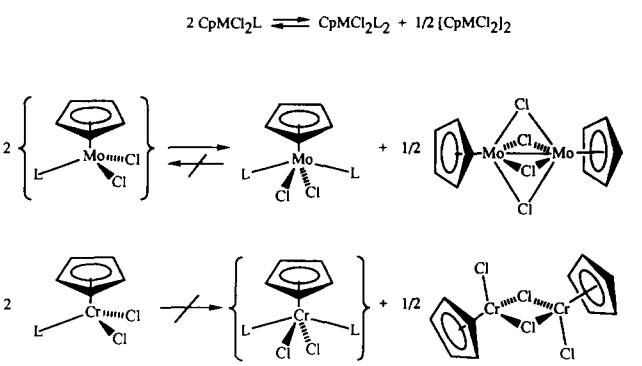

Scheme 1.

Table 4
Positional parameters and equivalent isotropic thermal parameters for $[Cp^*MoCl_2(PMe_2Ph)_2]AlCl_4$

Atom	x	y	z	B_{eq}
Mo	0.50501(4)	0.08476(7)	0.74667(3)	3.36(3)
Cl(1)	0.5968(1)	−0.0899(2)	0.7809(1)	4.7(1)
Cl(2)	0.4709(1)	0.3342(2)	0.7707(1)	5.3(1)
Cl(3)	0.1598(2)	0.4059(4)	0.9687(2)	12.3(3)
Cl(4)	0.1024(2)	0.0475(6)	0.9926(2)	13.5(3)
Cl(5)	0.2152(2)	0.1134(4)	0.8738(1)	8.9(2)
Cl(6)	0.2797(2)	0.1491(4)	1.0349(1)	8.3(2)
P(1)	0.4793(1)	0.0562(2)	0.8665(1)	3.8(1)
P(2)	0.6175(1)	0.2325(3)	0.7223(1)	4.7(1)
Al	0.1908(2)	0.1803(4)	0.9674(1)	5.8(1)
C(11)	0.5584(5)	0.103(1)	0.9172(4)	6.0(5)
C(12)	0.4125(5)	0.182(1)	0.8955(5)	5.9(5)
C(13)	0.4518(5)	−0.1271(9)	0.8941(4)	4.2(4)
C(14)	0.5018(5)	−0.242(1)	0.9043(4)	5.9(5)
C(15)	0.4799(7)	−0.382(1)	0.9247(5)	7.3(6)
C(16)	0.4118(8)	−0.404(1)	0.9379(5)	7.5(7)
C(17)	0.3610(6)	−0.294(1)	0.9292(5)	6.3(6)
C(18)	0.3819(5)	−0.156(1)	0.9078(4)	5.1(5)
C(21)	0.6839(5)	0.137(1)	0.6787(5)	6.4(5)
C(22)	0.6057(6)	0.406(1)	0.6779(5)	7.2(6)
C(23)	0.6636(5)	0.287(1)	0.7978(5)	5.2(5)
C(24)	0.6461(6)	0.420(1)	0.8288(5)	6.8(6)
C(25)	0.6795(8)	0.457(2)	0.8878(7)	8.7(9)
C(26)	0.7305(9)	0.363(2)	0.9156(6)	10(1)
C(27)	0.7509(7)	0.232(2)	0.8856(7)	9.1(8)
C(28)	0.7154(6)	0.199(1)	0.8285(5)	6.6(6)
C(31)	0.4900(5)	−0.063(1)	0.6536(4)	5.4(5)
C(32)	0.4460(5)	−0.1250(9)	0.6994(4)	4.4(4)
C(33)	0.3919(5)	−0.019(1)	0.7113(4)	5.5(5)
C(34)	0.4025(6)	0.107(1)	0.6717(5)	6.6(6)
C(35)	0.4634(6)	0.080(1)	0.6367(4)	6.1(5)
C(36)	0.5480(7)	−0.148(2)	0.6220(6)	10.3(8)
C(37)	0.4489(7)	−0.281(1)	0.7262(6)	8.8(7)
C(38)	0.3258(6)	−0.040(2)	0.7474(6)	11.0(9)
C(39)	0.3528(8)	0.238(2)	0.662(1)	15(1)
C(40)	0.486(1)	0.178(2)	0.5823(6)	15(1)

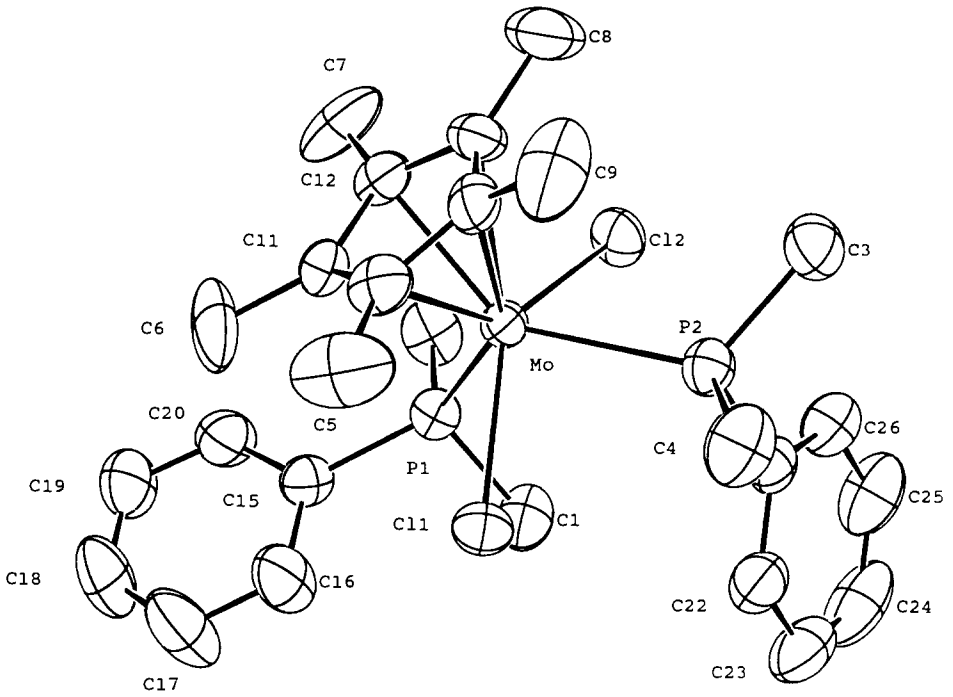

Fig. 2. An ORTEP view of the $Cp^*MoCl_2(PMe_2Ph)_2$ molecule with the atomic numbering scheme employed. Only the major orientation of the Cp^* ring is shown. Hydrogen atoms are omitted for clarity.

monodentate ligands and there is no metal–metal bond [10]. As a result, the equilibrium in the Scheme is shifted completely to the left.

The reaction between $Cp^*MoCl_2(PMe_2Ph)_2$ and $AlCl_3$ was carried out with the initial goal of abstracting a chloride ligand and generating a 15-electron [Cp^*Mo-

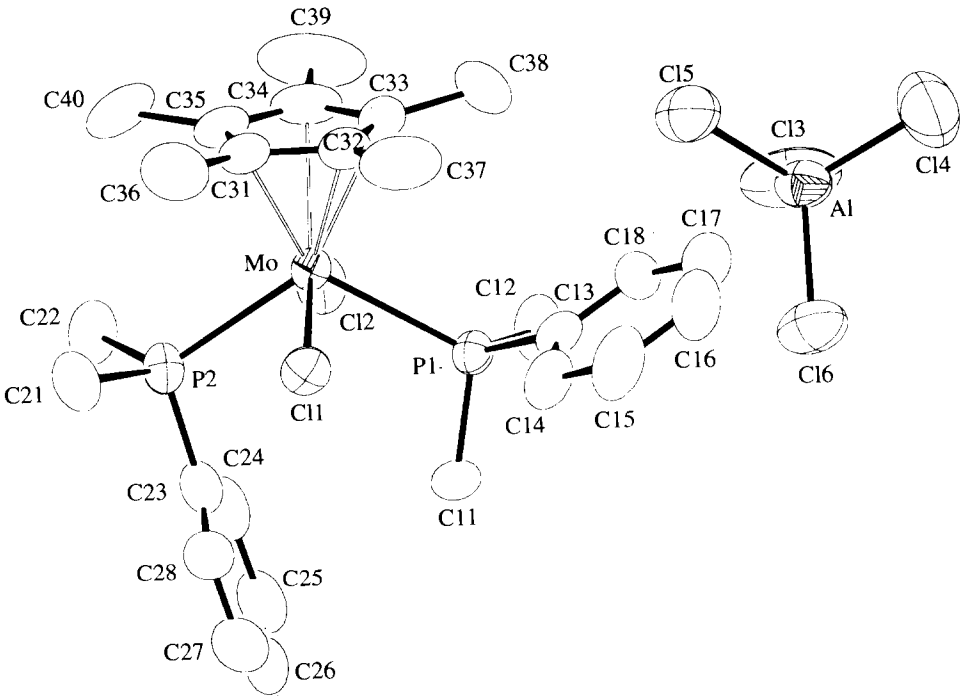

Fig. 3. An ORTEP view of the $[Cp^*MoCl_2(PMe_2Ph)_2]AlCl_4$ molecule with the atomic numbering scheme employed. The two fragments are shown in their correct relative orientation. Hydrogen atoms are omitted for clarity.

$Cl(PMe_2Ph)_2]^+$ derivative, which would be isoelectronic with analogous chromium compounds, e.g. $[Cp^*CrRL_2]^+$ (R = Me, Et; L = THF, py, PMe_3 or L_2 = bipy, dmpe, dppe) [11b]. We found that the 16-electron dichloride Mo(IV) complex, $[Cp^*MoCl_2(P-Me_2Ph)_2]^+$, was obtained in good yields instead, with the presumed participation of the CH_2Cl_2 solvent as indicated in Eqn. 5. This result is probably due to the facile oxidation of Mo(III) to Mo(IV), whereas the same tendency does not exist for chromium. It was previously shown that the one-electron oxidation of the Mo(III) $CpMoX_2(PMe_3)_2$ (X = Cl, Br, I) molecules is rather facile [5,20]. The cyclic voltammogram of $Cp^*-MoCl_2(PMe_2Ph)_2$ shows a reversible one-electron oxidation wave at −0.91 V vs. Cp_2Fe/Cp_2Fe^+ (cf. −0.84 V for $Cp^*MoCl_2(PMe_3)_2$ [20] and −0.55 V for $CpMo-Cl_2(PMe_2Ph)_2$ [7]) and a second oxidation wave at +0.88 V (cf. +0.84 V for $Cp^*MoCl_2(PMe_3)_2$ [20]). The potential shift in the negative direction as Cp^* replaces Cp (that is, the Cp^* derivatives are more easily oxidized than the corresponding Cp derivatives) is expected given the greater donor power of the Cp^* ligand.

$$Cp^*MoCl_2(PMe_2Ph)_2 + AlCl_3 \longrightarrow \{[Cp^*MoCl(PMe_2Ph)_2]^+AlCl_4^-\} \xrightarrow{CH_2Cl_2} [Cp^*MoCl_2(PMe_2Ph)_2]^+AlCl_4^- \quad (5)$$

The molecular geometries of compounds $Cp^*Mo-Cl_2(PMe_2Ph)_2$ and $[Cp^*MoCl_2(PMe_2Ph)_2]AlCl_4$ are shown in Figs. 2 and 3, respectively. The relevant intermolecular bond distances and angles are listed in Table 3. The neutral and cationic complexes exhibit the same four-legged piano stool geometry, with rather similar CNT–Mo–Cl and CNT–Mo–P angles (see Table 3). The trends in the bond distances on going from the neutral to the cationic complex parallel those previously observed for the $[CpMoCl_2(PMe_3)_2]^{n+}$ (n = 0, 1) pair of complexes [5]: the average Mo–Cl distance shortens by 0.097(3) Å, the average Mo–P distance *lengthens* by 0.039(11) Å, the Mo–CNT distance *lengthens* by 0.038(10) Å, the average P–C distance slightly shortens from 1.819[5] Å to 1.805[9] Å, and the average C–P–C angle increases from 101.9[7]° to 103.8[13]°. The significance of the latter changes increased when one separates the parameters related to the different kind of phosphine substituents; thus the average Me–P–Me angle increases from 101.2(2)° to 102.4(5)°, whereas the average Me–P–Ph angle increases from 102.2[6]° to 104.6[7]°. Furthermore, the η^5 configuration of the Cp^* ring is more distorted in the neutral Mo(III) complex (the difference between shortest and longest Mo–C bond is 0.140(7) Å, with respect to 0.051(11) Å in the cationic Mo(IV) complex).

As discussed previously [5], all these variations are consistent with the presence of significant Mo–P and Mo–Cp back-bonding in the Mo(III) species (which decreases or disappears upon oxidation to the Mo(IV) species), with the known electronic structure of this class of compounds [21] (which predicts an electronic configuration of the type $(xy)^2(z^2)^1$ for the Mo(III) complex) and with removal of one electron from the xy orbital upon oxidation to afford a paramagnetic (S = 1) Mo(IV) cation of configuration $(xy)^1(z^2)^1$. Since the xy orbital has (a) Mo–Cl π^* character, (b) $Mo-PMe_2Ph$ π character and (c) Mo–Cp^* δ character, removal of one electron from this orbital results, as expected, in (i) a strengthening of the Mo–Cl π bonding interaction (shortening of the Mo–Cl bond), (ii) a weakening of the $Mo-PMe_2Ph$ π interaction (lengthening of the Mo–P bond and opening of the R–P–R angles) [22] and (iii) a weakening of the Mo–Cp^* π interaction (lengthening of the Mo–CNT bond and rearrangement of the Cp^* ring to adopt [21] a more symmetric η^5 arrangement). The high-spin electronic configuration of the Mo(IV) complex (as opposed to the alternative $(xy)^2(z^2)^0$ configuration) is also indicated by the paramagnetically shifted ^{1}H-NMR spectrum of the compound. The isostructural and isoelectronic $Cp^*MoCl_3-(PMe_3)$ complex was shown by magnetic susceptibility measurements to be a Curie system with two unpaired electrons per metal atom [15]. The $AlCl_4^-$ ion in the structure of the Mo(IV) salt is almost perfectly tetrahedral with the highest deviation from the ideal tetrahedral angle being 2.7(2)°. The Al–Cl distance averages 2.111[11] Å.

The ^{1}H-NMR spectrum of the 17-electron $Cp^*Mo-Cl_2(PMe_2Ph)_2$ shows relatively broad resonances at 10.4, 7.9, 2.4 and −2.1 (see Fig. 1), consistent with the paramagnetism of the complex. Given the geometry of the compound, five resonances should be observed in a relative ratio of 15 (Cp^*):12 (Me):4 (o–Ph):4 (m–Ph):2 (p–Ph). Only four paramagnetically shifted resonances are observed, however, and their relative intensities are such that it is most reasonable to assign the most upfield-shifted one at δ −2.1 to the phosphine methyl protons and the other three resonances at δ 10.4, 7.9 and 2.4 to the *meta*, *ortho*, and *para* phenyl protons, respectively. The assignment of the *meta* and *ortho* resonances is tentative, and is based on the greater breadth of the 7.9 resonance, presumably because of the proximity to the paramagnetic center. No Cp^* resonance was observed within the ±100 ppm range. This finding was initially surprising since the analogous complex $Cp^*MoCl_2(PMe_3)_2$ has been reported [4] to display a ^{1}H-NMR resonance at δ −2.0 for the PMe_3 ligand (in good agreement with the resonance assigned by us to the same protons in the PMe_2Ph analogue) and a resonance at δ 41.2 for the Cp^* protons. Consequently, we have re-examined the ^{1}H-NMR spectrum of compound $Cp^*MoCl_2(PMe_3)_2$. We observe the PMe_3 resonance at ca. δ −2 but find

no trace of the reported Cp^* resonance at δ 41.2, nor any other broad resonance in the δ 20-100 region. On the other hand, an extremely broad resonance at ca. δ 15 ppm ($w_{1/2} > 2000$ Hz) is observable only for very concentrated solutions. This resonance, which we assign to the Cp^* protons, sharpens significantly upon warming (δ 13 ppm, $w_{1/2} = 1100$ Hz in C_6D_6 at 57°C, while the PMe_3 resonance is seen at -2.0 ppm with $w_{1/2} = 60$ Hz at the same temperature; the integration is correct at 57°C for $1Cp^*$ to $2PMe_3$ ligands). At lower temperature, the Cp^* resonance disappears in the background and the only observable resonance is that of the PMe_3 protons, which progressively broadens and shifts upon cooling [δ -3.3 ($w_{1/2} = 530$ Hz) at -22°C and δ -4.6 ($w_{1/2} = 1100$ Hz) at -71°C in d^6-acetone]. In the case of the corresponding *bis*-PMe_2Ph complex, warming the solution did not allow the unambiguous identification of a Cp^* resonance. This resonance should also be in the δ 10–20 region, but this region is overshadowed by the other sharper resonances. As for the origin of the reported [4] Cp^* resonance at δ 41.2 for $Cp^*MoCl_2(PMe_3)_2$, we can only suggest the possibility of a paramagnetic impurity [23].

For the 16-electron $[Cp^*MoCl_2(PMe_2Ph)_2]^+$ species, five broad ^{1}H-NMR resonances are observed, as expected, but a detailed assignment is not possible because the resonances are broader and more extensively overlapped compared with those for the Mo(III) complex. The only two unambiguous conclusions that can be drawn from this NMR experiment are that (i) the compound has a $S = 1$ ground state, and (ii) there is no impurity of the Mo(III) parent complex in the oxidized Mo(IV) material (the reverse is also true).

Acknowledgement

Acknowledgement is made to the Donors of the Petroleum Research Fund for support of this work through grant 25184-AC3. Additional support through awards from the NSF (PYI) and the Sloan Foundation is also gratefully acknowledged. We also thank Audrey A. Cole for measurements.

References and notes

[1] (a) P.W. Jolly, C. Krüger, C.C. Romão and M.J. Romão, *Organometallics, 3* (1984) 936;
(b) O. Andell, R. Goddard, S. Holle, P.W. Jolly, C. Krüger and Y.H. Tsay, *Polyhedron, 8* (1989) 203.

[2] (a) J.L. Davidson, K. Davidson and W.E. Lindsell, *J. Chem. Soc., Chem. Commun.*, (1983) 287;
(b) J.L. Davidson, K. Davidson, W.E. Lindsell, N.W. Murrall and A.J. Welch, *J. Chem. Soc., Dalton Trans.*, (1986) 1677.

[3] (a) M.L.H. Green, A. Izquierdo, J.J. Martin-Polo, V.S.B. Mtetwa and K. Prout, *J. Chem. Soc., Chem. Commun.*, (1983) 583;
(b) P.D. Grebenik, M.L.H. Green, A. Izquierdo, V.S.B. Mtetwa and K. Prout, *J. Chem. Soc., Dalton Trans.*, (1987) 9.

[4] R.T. Baker, J.C. Calabrese, R.L. Harlow and I.D. Williams, *Organometallics, 12* (1993) 163.

[5] S.T. Krueger, R. Poli, A.L. Rheingold and D.L. Staley, *Inorg. Chem., 28* (1989) 4599.

[6] S.T. Krueger, B.E. Owens and R. Poli, *Inorg. Chem., 29* (1990) 2001.

[7] R. Poli, B.E. Owens, S.T. Krueger and A.L. Rheingold, *Polyhedron, 11* (1992) 2301.

[8] R. Linck, B.E. Owens, R. Poli and A.L. Rheingold, *Gazz. Chim. Ital., 121* (1991) 413.

[9] (a) E.O. Fischer, K. Ulm and P. Kuzel, *Z. Anorg. Allg. Chem., 319* (1963) 253;
(b) D.Z. Tille, *Z. Naturforsch., 21b* (1966) 1239;
(c) A. Grohmann, F.H. Köhler, G. Müller and H. Zeh, *Chem. Ber., 122* (1989) 897.

[10] (a) F.H. Köhler, R. de Cao, K. Ackermann and J. Sedlmair, *Z. Naturforsch, 38b* (1983) 1406;
(b) D.B. Morse, T.B. Rauchfuss and S.R. Wilson, *J. Am. Chem. Soc., 110* (1988) 8234;
(c) F.H. Köhler, J. Lachmann, G. Müller, H. Zeh, H. Brunner, J. Pfauntsch and J. Wachter, *J. Organomet. Chem., 365* (1989) C15;
(d) D.B. Morse, T.B. Rauchfuss, S.R. Wilson, *J. Am. Chem. Soc., 112* (1990) 1860.

[11] (a) D.S. Richeson, J.F. Mitchell and K.H. Theopold, *J. Am. Chem. Soc., 109* (1987) 5868;
(b) B.J. Thomas and K.H. Theopold, *J. Am. Chem. Soc., 110* (1988) 5902;
(c) W.A. Herrmann, W.R. Thiel and E. Herdtweck, *J. Organomet. Chem., 353* (1988) 323;
(d) D.S. Richeson, J.F. Mitchell and K.H. Theopold, *Organometallics, 8* (1989) 2570;
(e) B.J. Thomas, S.K. Noh, G.K. Schulte, S.C. Sendlinger and K.H. Theopold, *J. Am. Chem. Soc., 113* (1991) 893.

[12] K. Angermund, A. Döhring, P.W. Jolly, C. Krüger and C.C. Romão, *Organometallics, 5* (1986) 1268.

[13] J.A. Barrera and D.E. Wilcox, *Inorg. Chem., 31* (1992) 1745.

[14] (a) M.W. Anker, J. Chatt, G.J. Leigh and A.G. Wedd, *J. Chem. Soc., Dalton Trans.*, (1975) 2639;
(b) J.L. Atwood, W.E. Hunter, E. Carmona-Guzman and G. Wilkinson, *J. Chem. Soc., Dalton Trans.*, (1980) 4657;
(c) F.A. Cotton and R. Poli, *Inorg. Chem., 26* (1987) 1514;
(d) B.E. Owens, R. Poli and A.L. Rheingold, *Inorg. Chem., 28* (1989) 1456;
(e) R. Poli and H.D. Mui, *Inorg. Chem., 30* (1991) 65;
(f) R. Poli and J.C. Gordon, *Inorg. Chem., 30* (1991) 30, 4550;
(g) R. Poli and J.C. Gordon, *J. Am. Chem. Soc., 114* (1992) 6723.

[15] F. Abugideiri, J.C. Gordon, R. Poli, B.E. Owens-Waltermire and A.L. Rheingold, *Organometallics, 12* (1993) 1575.

[16] R. Poli, B.E. Owens and R.G. Linck, *Inorg. Chem., 31* (1992) 662.

[17] R.C. Murray, L. Blum, A.H. Liu, and R.R. Schrock, *Organometallics, 4* (1985) 953.

[18] F. Abugideiri, G.A. Brewer, J.U. Desai, J.C. Gordon and R. Poli, *Inorg. Chem.*, in the press.

[19] K. Fromm and E. Hey-Hawkins, *Z. Anorg. Allg. Chem., 619* (1993) 261.

[20] R. Poli, B.E. Owens, and R.G. Linck, *J. Am. Chem. Soc., 114* (1992) 1302.

[21] P. Kubàcek, R. Hoffmann and Z. Havlas, *Organometallics, 1* (1982) 180.

[22] (a) A.G. Orpen and N.G. Connelly, *J. Chem. Soc., Chem. Commun.*, (1985) 1310;

(b) A.G. Orpen and N.G. Connelly, *Organometallics*, *9* (1990) 1206.

[23] The reduction of Cp^*MoCl_4 with Na/Hg (three equivalents) *under argon* in the presence of two equivalents of PMe_3 affords a solution which exhibits strong paramagnetically shifted resonances at δ 45 and δ 18, and no trace of the resonance resulting from $Cp^*MoCl_2(PMe_3)_2$. The nature of this paramagnetic product is currently under investigation. However, reduction of Cp^*MoCl_4 with Na/Hg (three equivalents) under argon in the presence of three equivalents of PMe_3 affords diamagnetic $Cp^*MoCl(PMe_3)_3$: F. Abugideiri, M.A. Kelland, R. Poli and A.L. Rheingold, *Organometallics*, *11* (1992) 1303.